

Spread of Venezuelan equine encephalitis virus in mice olfactory tract

A. B. Ryzhikov, E. I. Ryabchikova, A. N. Sergeev, and N. V. Tkacheva

Research Institute of Molecular Biology, State Research Center of Virology
and Biotechnology “Vector”, Kol'tsovo, Novosibirsk Region, Russia

Accepted June 14, 1995

Summary. Spread of Venezuelan equine encephalitis (VEE) virus and damage of the central nervous system (CNS) in mice infected by respiratory route was studied. Virus concentration in organs and blood, “dose-effect” relationships, and ultrastructural lesions in various tissues were examined in immune and normal mice. We showed, via three independent methods – characteristic curve investigations, tissue virus concentration dynamics, and ultrastructural methods – the spread of VEE virus through the olfactory tract into the brain of immune mice. From these experiments it was concluded that in case of respiratory challenge VEE virus can enter the CNS of normal mice by both vascular and olfactory pathways, while in immune mice the main route is olfactory.

Introduction

An understanding of the pathways by which neurotropic viruses may enter the CNS is important for the analysis of the possible pathogenic mechanisms of these infections. Three probable mechanisms of virus conveyance into the CNS have been postulated: 1. vascular route involving crossing the blood-brain barrier and entering the CNS; 2. neurogenic spread along the peripheral nerves; and 3. olfactory pathway, which begins from the infected olfactory neuroepithelial cells [1]. The possibility of viral entry into the brain by means of olfactory neuroepithelial cells infection has been shown for Venezuelan equine encephalitis (VEE) virus [7–10, 12–13, 19], St. Louis virus [16], herpes simplex virus [6, 14] and mouse hepatitis virus [21], and is assumed for some other viruses. Some findings could be indirect evidence in favour of an assumption that the immune barrier is weaker along the olfactory pathway [15, 17]. In [4, 5] the existence of macromolecular transport along the olfactory nerve has been shown.

Knowledge of the mechanisms of the olfactory route of infection may be helpful for the following modes of interference with infection: 1. the intranasal application of drugs for blocking viral spread along the olfactory tract; 2. the

transport of drugs along the olfactory pathway into the CNS; 3. the possibility of local immunization of the olfactory zone for the effective prevention of CNS viral infection.

In our study we tried to investigate the entry of VEE virus into the brain of respiratory infected immune and normal mice and to determine the significance of the olfactory tract in development of CNS damage.

Materials and methods

Mice

Outbred ICR mice weighing 18–20 g were used. They were obtained from the colony of the State Research Center (SRC) “Vector” (Russia).

Virus

The Trinidad (IA) strain pathogenic for humans and the attenuated TC-83 strain [2] of VEE virus were obtained from the DI Ivanovsky Institute of Virology. Strains were passed twice through chicken embryos and once through Vero cells. Culture fluid containing virions at a concentration of 3×10^8 pfu/ml was collected from infected Vero cells. Virus samples were stored at -20°C before use.

Aerosol challenge

Exposure of animals to virus aerosols was carried out in a dynamic aerosol system with horizontal aerosol flow. The velocity of flow was 10 cm/sec, and airflow through the system was 20 l/min. The mass median diameter of the particles generated was 0.95 μm . The mice were exposed to the aerosol for 2 min, and the aerosol was sampled over the whole of this period using impingers like aerosol samplers containing 10.0 ml Earle’s solution obtained from SRC Vektor supplemented with 2% bovine serum (SRC Vektor), 100 units/ml of penicillin and 100 mcg/ml of streptomycin (“KrasnoiarSKmedpreparaty”). The respiratory dose was calculated on the basis of the virus aerosol concentration and the mouse minute respiratory volume of mouse using the Guyton formula [11]. 600 normal and 210 immune mice were used for determination of “dose-effect” relationships in aerosol challenge experiments.

Animal inoculation and immunization

Local intranasal route was realized by inoculation of virus suspension into the olfactory zone by inserting a blunt needle into a nostril of the anaesthetized mouse. The needle length corresponded to the distance between the nostril and the olfactory zone. Inoculum volume was about 1 μl . Nasomucosal damage did not occur. This method of infection provided the ratio of virus quantity in the nose to the virus quantity in the lungs about 100:1, as was defined by virus assay and radioisotope methods. 510 normal and 220 immune mice were used for determination of “dose-effect” relationships in local intranasal challenge experiments.

Subcutaneous mice inoculation was made by injection of 0.2 ml virus suspension. 230 normal and 230 immune mice were used.

Immunization of mice was performed by subcutaneous injection of 0.2 ml rabbit immune serum to produce a specific antibody titre of 1:200–1:300 as determined in radioimmunoassays. This route of immunization provided the least dispersion of immune antibody levels in blood of experimental animals. Only passively immunized mice were used for

determination of tissue virus concentration, in the ultrastructural studies, and in the “dose-effect” experiments.

Tissue sampling

Virus distribution in mouse organs was determined at different intervals after respiratory inoculation. Anaesthetized mice were perfused with 200–300 ml Earle’s solution supplemented with antibiotics. The degree of perfusion was controlled by measuring the hemoglobin concentration in suspensions of homogenized organs. Hemoglobin concentration was diminished more than 100 times by this technique. The presence of virus at various time intervals postinfection was defined in organs of three mice at each time point of experiments. Tissue specimens were homogenized, and 10% suspensions of tissue in Earle’s solution with 2% bovine serum and antibiotics were stored at -20°C before titration. Tissue samples for ultrastructural analysis were obtained at the same time from nonperfused animals.

Virus assay

VEE virus concentrations were defined by plaque assay procedures. Chick embryo fibroblast cell monolayers in glass bottles were inoculated with 0.2 ml of viral suspension. After 1 h at 37°C , the maintenance medium containing 2.4% agar (Difco) and 0.001% neutral red (Merck) was added to the bottles. Cells were incubated in a dark room during 48 h at 37°C , and plaques were counted. Control of sensitivity of cell monolayers was performed by the TC-83 strain that was stored at -20°C .

Statistical analysis

Method of maximal probability was applied for estimation of $\lg\text{LD}_{50}$ (median) and b (slope) [3]. These values were parameters of alternative “dose-effect” relationship. We supposed the log-normal nature of distribution of individual animal sensitivity to infection [18]. Parameter b that characterized the slope of “dose-effect” relationship in log-normal axis was calculated as a value inversely proportional to the deviation of animal sensitivity distribution. LD_{50}^* and LD_{50} are 50% lethal doses for immune and normal mice respectively. Testing of H_0 -hypothesis for parameters $\lg\text{LD}_{50}$ and b for various animals groups was carried out by standard normal variable quantity (z -statistics) with statistical assurance (S) 95% [18]. The resistance index (IR) was calculated as $\text{IR} = \lg\text{LD}_{50}^* - \lg\text{LD}_{50}$.

Electron microscopic studies

Tissue specimens for ultrastructural study were obtained at 24, 36, 48, 72 h postinoculation, fixed in a 4% paraform aldehyde and 2.5% glutaraldehyde solution and postfixed in 1% osmium tetroxide solution. The material was dehydrated and embedded in Epon-Araldite (Serva). Ultrathin and semithin sections were cut upon a Reichert (Reichert-Young, Austria) ultratome and were contrasted with uranyl acetate and lead citrate. Semithin sections were stained with azur-2 (Serva). Thin sections were examined in H-600 (Hitachi, Japan) and JEM – 100S (JEOL, Japan) electron microscopes.

Results

For detailed characterization of virus-animal interactions we examined the “dose-response” dependence as well as the $\lg\text{LD}_{50}$ and b (the slope of a “dose-response” relationship straight lines in log-normal axes) [18].

The results for the challenge of normal and immune mice are given in Table 1. The values of $\lg LD_{50}$, b and IR for various methods of inoculation could be estimated. It should be noted that the characteristic curves for normal and immune mice have different slopes (b) for the same challenge mode. Parameters b differed in the cases of aerosol, subcutaneous and intranasal challenge of normal mice with statistical assurance more than 95%. The same parameters in immune mice decreased and did not differ for different inoculation routes ($S > 95\%$). Thus, despite of equal levels of injected immune antibodies in mice we registered widening of distribution of individual sensitivities of animals to virus (b value diminished).

$\lg LD_{50}$ value for normal mice increased in aerosol infection ($\lg LD_{50\text{aero}} = 0.23$) and olfactory zone challenge ($\lg LD_{50\text{i/n}} = 2.07$), as compared with subcutaneous infection ($\lg LD_{50\text{s/c}} = -0.32$), whereas in immune mice $\lg LD_{50\text{aero}}^* = 2.56$ increased to $\lg LD_{50\text{i/n}}^* = 3.39$ and then to $\lg LD_{50\text{s/c}}^* = 3.78$.

The resistance index (IR) falls about three times upon a change from subcutaneous challenge ($IR = 4.1$) to aerosol ($IR = 2.3$) and intranasal olfactory zone challenge ($IR = 1.3$). These data demonstrated that the olfactory tract represented a way for viral propagation weakly controlled by host immunity.

Dependence of VEE virus concentrations in blood and tissues of infected immune and normal mice of the time after respiratory challenge show further evidence in support of the importance of the olfactory zone in the pathogenesis of VEE virus infection. The infectious dose was chosen to secure 100% mice lethality and to produce a low rate of virus concentration rise in animal tissues. Dependence of VEE virus concentrations in blood and tissues in immune and normal mice of the time after respiratory challenge is shown in Fig. 1, where each point represents the average value of virus concentration in the organs of three mice. VEE virus concentrations were assayed in brain, olfactory bulbs, olfactory zone of nose, throat, trachea, lungs, blood, liver, spleen, kidney, adrenal glands,

Table 1. $\lg LD_{50}$ and b values for various routes of inoculation of normal and immune mice with Venezuelan equine encephalitis virus

Inoculation route	$\lg LD_{50}$	SD_L	b	SD_b	$\lg LD_{50}^*$ ^a	SD_L^* ^b	b^{*c}	SD_b^{*d}	IR^e
Intranasal	2.07	0.13	0.64	0.05	3.39	0.22	0.38	0.06	1.3
Aerosol	0.23	0.05	1.28	0.10	2.56	0.29	0.47	0.11	2.3
Subcutaneous	-0.32	0.14	0.86	0.11	3.78	0.32	0.47	0.06	4.1

^a LD_{50} , LD_{50}^* 50% lethal doses in plaque forming units for normal and immune mice respectively

^b SD_L , SD_L^* Standard deviation of parameters $\lg LD_{50}$ and $\lg LD_{50}^*$ respectively

^c b , b^* Slope of "dose-effect" relationship in log-normal axis for normal and immune mice respectively

^d SD_b , SD_b^* Standard deviation of parameters b and b^* respectively

^e IR Resistance index

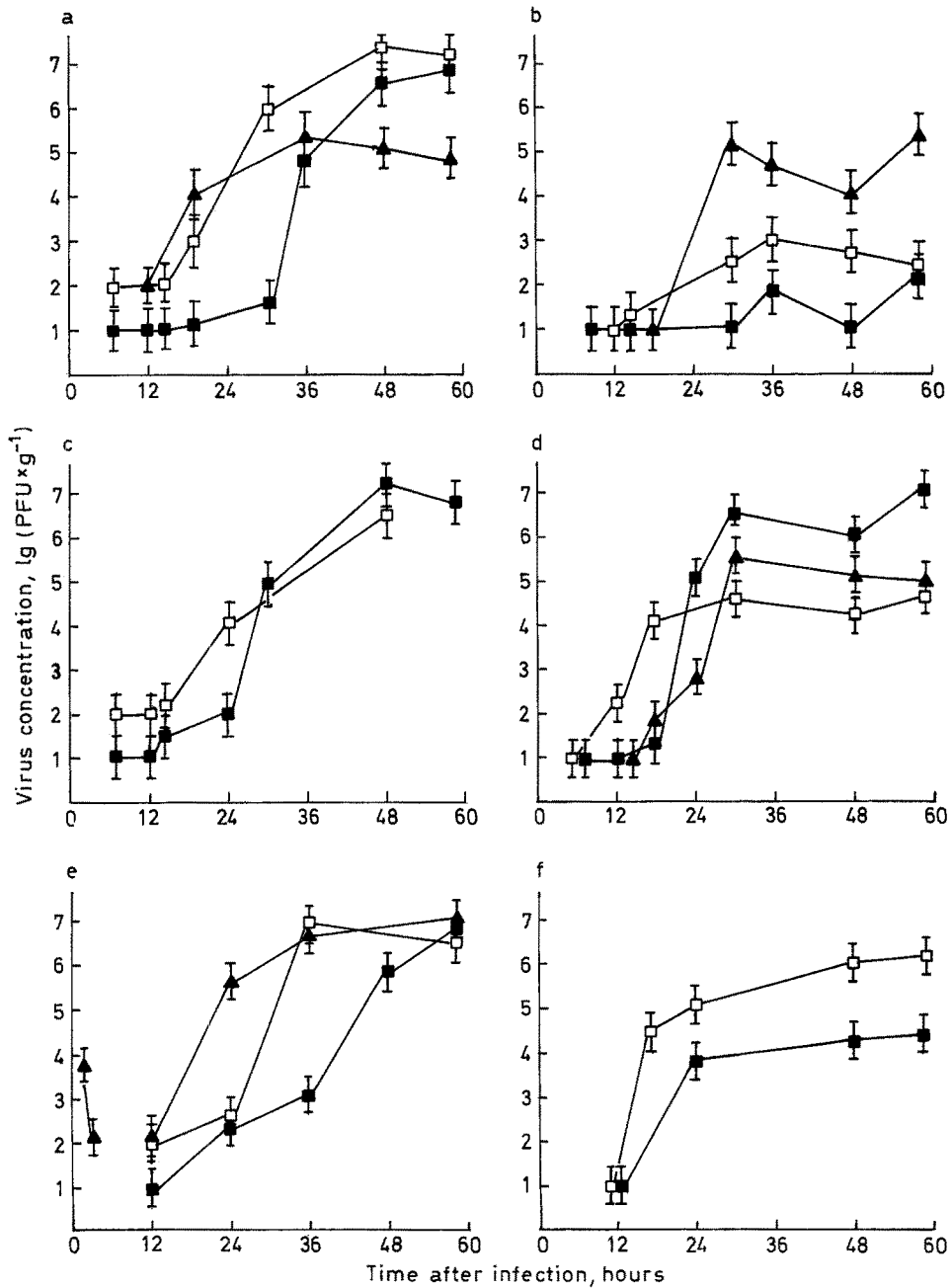


Fig. 1. VEE virus concentration in organs and tissues of normal and immune mice versus time after respiratory infection. **a, b** Aerosol challenge of immune mice (challenge dose 2.5 lg(PFU)); **c, d** aerosol challenge of normal mice (challenge dose 3.0 lg(PFU)); **e, f** intranasal (locally onto olfactory zone) challenge of normal mice (challenge dose 2.5 lg(PFU)). **a, c, e** - \square - olfactory bulb, - \blacksquare - brain, - \blacktriangle - olfactory zone, **b, d** - \square - lung, - \blacksquare - blood, - \blacktriangle - spleen, **f** - \square - blood, - \blacksquare - lung

bone marrow, lymph nodes, heart. The graphs in Fig. 1 are illustrative of the role of the olfactory tract in the development of virus brain infection.

Virus appeared first in the lungs of normal mice, then in blood and other tissues (Fig. 1c, 1d). Between 16 h and 24 h after aerosol challenge virus concentration in olfactory bulb was about 3 orders greater than in brain. The two values then became equal and rose to 10^7 PFU/g at 60 h after the challenge. The concentration in the blood was 10^6 – 10^7 PFU/g at that time.

In aerosol infected immune mice virus appeared first in the olfactory zone, lung and olfactory bulb (Fig. 1a, curves – □ –, – ▲ –, Fig. 1b, curve – □ –). Virus concentration in the lungs was reduced (10^3 PFU/g) in comparison with normal mice. Virus was detected in the olfactory zone of the nose and olfactory bulb on 20 h postinfection at concentrations of 10^3 – 10^4 PFU/g. The same virus concentration in brain were reached only 12–14 h later. After 36 h the blood virus was found at relatively low concentrations (10^2 PFU/g).

Concentration curves observed in the brain branches and olfactory zone in immune mice after aerosol challenge were similar to those found after intranasal dosage of normal mice (Figs. 1e, 1f). In the latter case virus appeared first in the olfactory zone, then in blood, and later in the lungs at 10^4 PFU/g.

Ultrastructural data were consistent with the results of the virological study and demonstrated the propagation of VEE virus in nasal mucous after local intranasal inoculation onto the olfactory zone. Virus-induced changes were observed at 20 h postinfection both in olfactory epithelium and in olfactory bulb. Degenerative changes were registered in neuroepithelial cells, supporting cells and basal cells, and in mucosal lamina propria including Bowman's glands, which produce specific secretion for the olfactory epithelial surface.

Morphological features of virus reproduction were seen at 48 h after inoculation both in olfactory epithelium cells and in secretory cells of Bowman's glands (Fig. 2). Infected cells contained virus-specific structures: osmiophilic amorphous aggregates of viroplasm, spherical nucleocapsids 28 nm in diameter with a lucent center 10 nm in diameter and mature virions 55 nm in diameter in cisternae of the Golgi apparatus and in vacuoles. Virus budding was observed on the membranes of the Golgi apparatus and on the plasma membrane. In addition, mature virions were present in secretory granules of Bowman's gland cells. These findings were not unexpected because secretory granules developed from the Golgi apparatus. Unusual tubular structures 18 nm in diameter situated in the lumen of the endoplasmic reticulum were registered in infected cells. The role of these tubules was not clear, but they did not appear to be directly connected with virion formation. VEE virus reproduction was not found in polymorphs, vascular endothelium, and cells of lamina propria connective tissue. Only neurons and Bowman's gland cells were capable to VEE virus reproduction.

Alteration and necrosis of epithelial and Bowman's gland cells, polymorph infiltration of the olfactory epithelium and lamina propria of nasal mucosa was observed in the olfactory zone of mice at 48 h after intranasal inoculation. The olfactory nerve always contained few degenerating axons, and VEE virus particles were found between them.

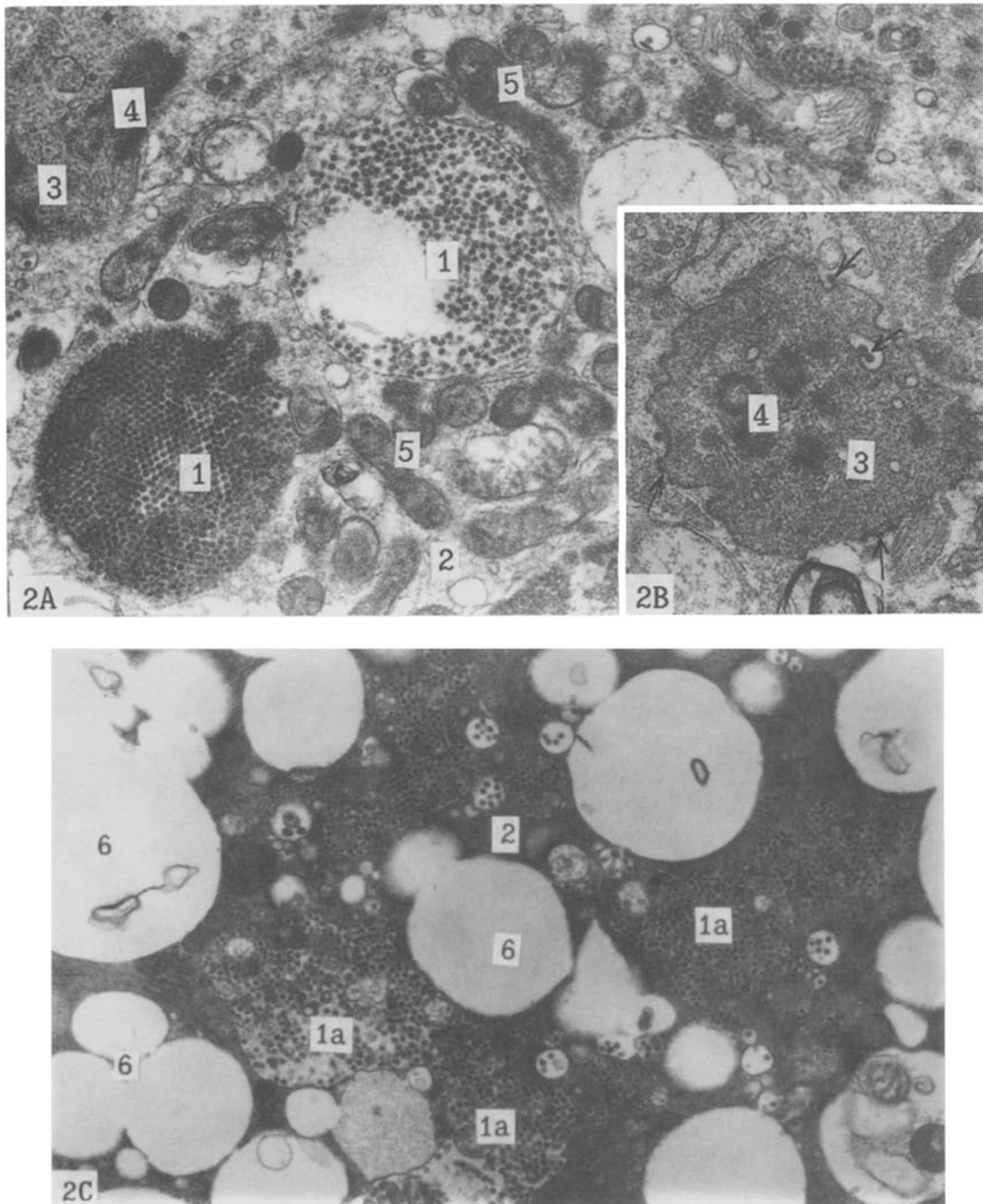


Fig. 2. VEE virus reproduction in nasal mucous, 48 h after inoculation onto olfactory epithelium. **A** Sustentacular cell of olfactory epithelium. **B** Viral budding on plasma membrane of olfactory mace (arrows); **C** Bowman's gland cell. $\times 20000$. 1 Congestion of viral particles in vacuoles and secretory granules (1a); 2 cytoplasm; 3 part of olfactory mace; 4 lash; 5 mitochondria; 6 secretory granules free of virions

Comparative studies of olfactory bulbs and brain cortex showed that virus reproduction and histopathological changes appeared in the olfactory bulbs earlier than in brain cortex. Morphological evidence of viral reproduction (Fig. 3)

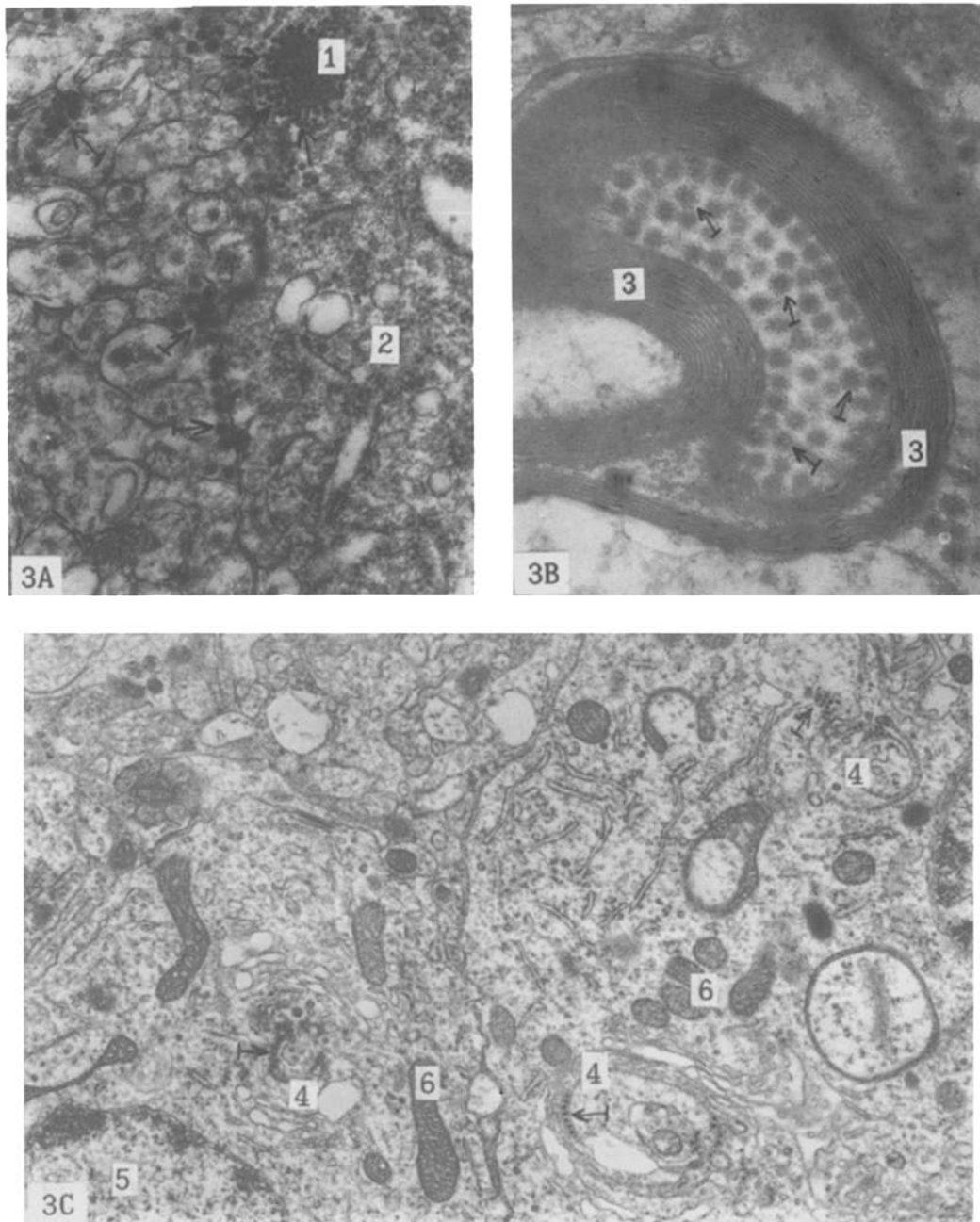


Fig. 3. Olfactory bulb of mice, 48 h after aerosol inoculation of VEE virus. **A** VEE reproduction in neuron. $\times 40\,000$. **B** VEE viral particles within the myelinated nerve fib. $\times 80\,000$. **C** Two infected neurons. $\times 15\,000$. 1 Viroplasm; 2 cytoplasm; 3 myelinated envelope of axon; 4 Golgi apparatus; 5 nucleus; 6 mitochondria; arrows: nucleocapsids; stressed arrows: virions

was observed in all cell types of nerve tissue. A significant amount of morphologically mature virions was concentrated inside the cells, in the cisterns and vacuoles of the Golgi apparatus. Mature virions were found also in myelinated axons. Virions can probably spread from olfactory bulb neurons into the CNS via axonal transport. Several pathological changes were noted at the border peripheral part of the olfactory bulb affecting a layer of large neurons and surrounding glial cells as early as 48 h after respiratory inoculation. Zones of injury were characterized by erythrocyte congestion and little haemorrhages, polymorph infiltration, and oedematous or necrotic lesions of nerve cells and neuropili.

Pathological changes in brain cortex were registered only at 72 h after respiratory inoculation. Mononuclear infiltration of neural parenchyme and perivascular regions (so-called perivascular cuffs) was observed in brain cortex. We observed damaged endothelial cells, erythrocytes congestion and haemorrhages. Destructive changes of cortical nervous tissue (oedema, necrosis) were usually perivascular. Injured zones were mostly infiltrated by mononuclear cells and polymorphs; many macrophages with a large phagosomes were found in the same zones 96 h postinoculation. Reproduction of VEE virus was seen only in few damaged cortex zones. The number of infected cells and viral particles were far less than were observed in the slices of the olfactory bulb. This phenomenon was probably connected with mechanisms inhibiting virus reproduction some time after inoculation. Perhaps mononuclear infiltrating cells participate in these inhibition mechanisms.

Discussion

Differences in the parameters of $lgLD_{50}$ and b and virus concentration after VEE virus infection are indicative of the specific sensitivity of the olfactory pathway.

VEE virus in aerosol challenged normal mice was detected first in lung, secondly in blood, and later in other organs including the olfactory bulb (Figs. 1c, d). From the blood stream virus may enter the CNS through blood-brain barrier, which formed with uninterrupted capillary epithelium and provided the extremely low penetration of an infectious agent into the CNS. Only in the olfactory neuroepithelium zone the uninterrupted endothelium changed to a fenestrated one which is specific for secretory tissues (Bowman's gland cells). The diameter of the fenestrae between endothelial cells is about 0.1 μ m [1]. This structure of capillaries could allow closer interaction between virus and sensitive neuroepithelial cells. These anatomical peculiarities allow the indirect infection of olfactory zone nerve terminals from blood stream through nasal mucous.

We observed a high level of protection produced by immune serum in mice, subcutaneously injected with VEE virus, which was much less in the case of aerosol and intranasal challenge (Table 1). These results imply the possibility of direct infection of neuroepithelial cells by viral aerosol particles impacted on nasal mucous. The VEE virus concentration in blood of immune mice was very low (Fig. 1b). Direct infection of nerve terminals in olfactory zone of nasal cavity

is the predominant factor in development of CNS damages (Fig. 1a). Absence of differences between $\lg LD_{50}$ and parameter b ($S > 95\%$) in aerosol and intranasal infected immune mice confirmed this supposition. Passive immunization smoothed the differences of immune antibodies levels and diminished the role of blood-brain barrier. The significance of olfactory tract in VEE virus spread markedly rose in this case. Hence, individual peculiarities of olfactory tract in immune mice became more prominent and influence on the widths of animals sensitivities distribution (b value diminished) (Table 1).

Our data provide reasons enough to assume direct infection of neuroepithelial cells with VEE virus, and viral entrance into the CNS through the olfactory tract. This view is supported by the results of ultrastructural investigations and the concentrations of virus in various organs (Figs. 1–3). Jahrling and Stephenson [13] supposed that local immunity of the olfactory zone was very significant in the protection of hamsters against VEE virus aerosol infection, and our findings in mice support them.

Parameters $\lg LD_{50}$ of “dose-effect” relationships (Table 1) illustrated the various sensitivity of animals for different inoculation methods. Normal mouse sensitivity for aerosol infection is two orders greater than that registered in the experiments with intranasal inoculation. In the case of aerosol challenge synchronous infection of the upper and lower parts of respiratory tract developed. The values of LD_{50} for normal mice in our aerosol exposure experiments are in a good agreement with the results of Stephenson et al. [20].

Ultrastructural investigation revealed VEE virus reproduction in olfactory epithelium and in the Bowman’s glands of the lamina propria. Therefore infection of the nasal mucous olfactory zone suggests two possible routes of viral spread: 1. through the fenestrated epithelium of olfactory zone capillaries allowing entry of viral particles into the blood stream with subsequent spread of infection, 2. transport along the olfactory nerve with viral penetration into the olfactory bulbs and spread to the CNS.

Our data showed some new features of VEE virus morphogenesis. VEE virions accumulated in vacuoles of the Golgi apparatus of neural and Bowman’s gland cells. Such connection of Golgi apparatus and VEE virus morphogenesis was not reported [8]. Virions, packed in vacuoles, can move along the axons by the same mechanisms which serve for cellular organelle transport. A mechanism of rapid axonal transport can quickly deliver virus directly into the olfactory bulb. It is very important that virions remain inside the cell during this spread and have no contact with the extracellular medium. Consequently the virus is inaccessible for inactivation by antibodies.

In summary, our complex investigation showed the spread of VEE virus through the olfactory tract into the brain in immune mice. We suppose the exploitation of the olfactory tract for the entrance into the CNS by viruses that could not produce high concentrations in blood [16] or low-virulence viruses [15, 21]. Two questions arise: is it the main pathway for other animal species, and can the olfactory application of drugs and vaccines protect the CNS against virus damage? These problems will be examined in future research.

References

1. Albrecht P (1968) Pathogenesis of neurotropic arbovirus infection. *Curr Top Microbiol Immunol* 43: 44–91
2. Berge T, Banks I, Tigertt W (1961) Attenuation of Venezuelan equine encephalitis virus by in vitro cultivation in guinea pig heart cells. *Am J Hyg* 73: 209–211
3. Borovkov AA (1984) *Matematicheskaya statistika (Mathematical statistics)*. Nauka, Moskva [in Russian]
4. Cancalon P, Brady ST, Lasek RJ (1988) Slow transport in a nerve with embryonic characteristics, the olfactory nerve. *Dev Brain Res* 38: 275–285
5. Cole GJ, Elam JS (1983) Characterization of axonally transported glykoproteins in regenerating garfish olfactory nerve. *J Neurochem* 41: 691–702
6. Cook ML, Stevens JG (1973) Pathogenesis of herpetic neuritis and ganglionitis in mice. *Infect Immun* 7: 272–288
7. Danes L, Kufner J, Hruskova J, Rychterova V (1973a) The role of olfactory pathway in respiratory tract VEE infection of normal and operated *Macaca rhesus*. I. Results of virological studies. *Acta Virol* 17: 50–56 [in Russian]
8. Danes L, Rychterova V, Kliment V, Hruskova J (1973b) Penetration of Venezuelan equine encephalitis virus into the brain of guinea pigs and rabbits after intranasal inoculation. *Acta Virol* 17: 138–146 [in Russian]
9. Davis NL, Grieder FB, Smith JF, Greenwald GF, Valenski ML, Sellon DC, Charles PC, Johnston RE (1994) A molecular genetic approach to the study of Venezuelan equine encephalitis virus pathogenesis. In: Brinton MA, Calisher CH, Rueckert RR (eds) *Positive-strand RNA viruses*. Springer, Wien New York, pp 99–109 (*Arch Virol* [Suppl] 9)
10. Grimley PM, Berezsky SK, Friedman RM (1968) Cytoplasmic structures associated with arbovirus infection: foci of viral ribonucleic acid synthesis. *J Virol* 2: 1326–1338
11. Guyton AC (1947) Measurement of respiratory volumes of laboratory animals. *Am J Physiol* 150: 70–77
12. Jackson AC, SenGupta SK, Smith JF (1991) Pathogenesis of Venezuelan equine encephalitis virus infection in mice and hamsters. *Vet Pathol* 28: 410–418
13. Jahrling PB, Stephenson EH (1984) Protective efficacies of live attenuated and formaldehyde-inactivated Venezuelan equine encephalitis virus vaccines against aerosol challenge in hamsters. *J Clin Microbiol* 19: 429–431
14. Johnson RT (1964) The pathogenesis of herpes virus encephalitis. I. Virus pathways to nervous system of suckling mice demonstrated by fluorescent antibody staining. *J Exp Med* 119: 343
15. Kaluza G, Lell G, Reinacher M, Stits L, Willems WR (1987) Neurogenic spread of Semliki Forest virus in mice. *Arch Virol* 93: 97–110
16. Monath TP, Cropp CB, Harrison AK (1983) Mode of entry of a neurotropic arbovirus into the central nervous system. Reinvestigation of an old controversy. *Lab Invest* 48: 399
17. Reinacher M, Bonin J, Narayan O, Scholtissek C (1983) Pathogenesis of neurovirulent influenza A virus infection in mice. Route of entry of virus into brain determines infection of different populations of cells. *Lab Invest* 49: 686–692
18. Sachs L (1972) *Statistische Auswertungsmethoden*. Springer, Berlin Heidelberg New York
19. Sergeev AN, Ryzhikov AB, Bulychev LE, Stepkina EO, Tkacheva NV (1991) *Techenie infektsii u krolikov, aerogenno zarazhennykh virusom venesuel'skogo entsefalomielitja loshadei (The course of airborne infection in rabbits infected with the Venezuelan encephalomyelitis virus)*. *Vopr Virusol* 36: 492–495 [in Russian]

20. Stephenson EH, Moeller RB, York CG, Young HW (1988) Nose-only versus whole-body aerosol exposure for induction of upper respiratory infections of laboratory mice. *Am Ind Hyg Assoc J* 49: 128–135
21. Taguchi F, Goto Y, Aiuchi M, Hayashi T, Fujiwara K (1979) Pathogenesis of mouse hepatitis virus infection. The role of nasal epithelial cells as a primary target of low-virulence virus, MHV-S. *Microbiol Immunol* 23: 249–262

Authors' address: Dr. A. B. Ryzhikov, Research Institute of Molecular Biology, State Research Center of Virology and Biotechnology "Vector", 633159 Kol'tsovo, Novosibirsk Region, Russia.

Received August 24, 1994